Theory of the excitonic optical Stark effect
in quasi-one-dimensional semiconductor quantum wires

Nguyen Ba An* and Hartmut Haug

Institut für Theoretische Physik, J. W. Goethe Universität Frankfurt, Robert-Mayer-Strasse 8, D-6000 Frankfurt am Main, Germany

The nonresonant excitonic optical Stark effect is calculated for quasi-one-dimensional semiconductor quantum wires up to first order in the pump intensity. For quasistationary situations a large blueshift with an oscillator strength that decreases with pump intensity is predicted. This result is due to the dominance of the phase-space filling effect in quantum wires and is in striking contrast with results for corresponding three-dimensional (3D) and 2D systems.

I. INTRODUCTION

The increase of the exciton binding energy in low-dimensional systems in comparison with that in bulk material allows the observation of excitonic effects even at room temperature. This, together with recent progress in crystal-growth techniques of various quantum confined systems, has led to an intensive investigation of semiconductor quantum wells, quantum wires, and quantum dots.[1] Parallel advances in ultrashort-pulse spectroscopy methods made it possible to observe coherent optical processes in semiconductors.[2] Examples are the observation of the optical Stark effect, of quantum beats, and of the photon echo in bulk and quantum-well semiconductors.

In this work we will calculate the nonresonant excitonic optical Stark effect in a quasi-one-dimensional (Q1D) system, i.e., in a semiconductor quantum wire. We follow corresponding theories for 3D and 2D structures.[3−7]

Since the pioneering work of Loudon[8] on a one-dimensional hydrogen atom, many papers have been concerned with different aspects in semiconductor quantum wires, such as the exciton or biexciton binding energies and connected nonlinearities,[9,10] band-to-band absorption,[11,12] carrier-induced optical nonlinear effects,[13−15] etc.

Our paper is organized as follows. In Sec. II we recapitulate the general formulation of the nonresonant excitonic optical Stark effect, which is then applied in Sec. III to the calculation of the level shifts and the total oscillator strength in semiconductor quantum wires. In Sec. IV a comparison of our Q1D results with corresponding results for 2D and 3D systems is given.

II. GENERAL FORMULATION
OF THE OPTICAL STARK EFFECT

Consider a direct-band-gap semiconductor with the renormalized conduction- and valence-band energies ϵ_{ck} and ϵ_{vk} which is externally pumped by a coherent radiation field of amplitude E_p and frequency ω_p. Denote by a_{ck} (a_{ck}^+) and a_{vk} (a_{vk}^+) the annihilation (creation) operators of the electron in the conduction and valence bands, respectively. The stationary equations of motion for the interband polarization operator $\pi_k = \langle a_{ck}^+ a_{vk} \rangle$ and for the density operators of the electrons in the conduction and valence bands $n_{ck} = \langle a_{ck}^+ a_{ck} \rangle$ and $n_{vk} = \langle a_{vk}^+ a_{vk} \rangle$, can be derived easily in the Hartree-Fock approximation, taking into account the presence of the pump field[1,5] alone (the units used throughout this paper are $\hbar = c = 1$):

$$(\epsilon_{ck} - \epsilon_{vk} - \omega_p)\pi_k = (1 - 2n_k) \left[d_{cv}E_p + \sum_{k'} V_{k-k'}\pi_{k'} \right] , \tag{1}$$

where

$$n_k \equiv n_{ck} = 1 - n_{vk} = \tfrac{1}{2}[1 - (1 - 4|\pi_k|^2)^{1/2}] \tag{2}$$

and

$$\epsilon_{ik} = \pm E_g/2 \pm \frac{k^2}{2m_i} \pm \sum_{k'} V_{k-k'}n_k . \tag{3}$$

Here the prefactor $(1 - 2n_k)$ in the right-hand side of (1) accounts for the phase-space filling (PSF) effect while E_g is the band gap, $V_{k-k'}$ is the Coulomb potential, and d_{cv} is the interband electric dipole matrix element. In general, π_k and n_k depend on time that requires a fully quantum kinetics treatment and the coupled equations (1) and (2) form a complicated set of nonlinear integral equations. However, in a nonresonant regime and at low pumping intensities one can develop a linear-response theory in which $n_k \simeq |\pi_k|^2 \propto |E_p|^2$. Then perturbation theory can be used that allows us to expand π_k in terms of a series of unperturbed exciton wave functions $\psi_n(k)$ as

$$\pi_k = \sum_n C_n \psi_n(k) . \tag{4}$$

The pump-field-induced polarization is in lowest order

$$\pi_k^p = d_{cv}E_p \frac{\Psi_n^*(r=0)\psi_n(k)}{\omega_n^{(0)} - \omega_p - i\delta} , \tag{5}$$

where $\psi_n(r)$ is the exciton wave function in real space.

The pump-field-induced effects, i.e., the optical Stark effect, can be measured with a weak resonant test field E_t with a frequency ω_t. Linearizing the polarization $\pi_k = \delta\pi_k^t + \pi_k^p$ in the presence of both the weak test field and the stronger pump field, one finds up to second order in the pump field the following optical susceptibility for the test beam $\chi(\omega_t)$ (for details, see, e.g., Refs. 1, 5, and 7):

$$\chi(\omega_t) = 2\sum_n \frac{f_n}{\omega_n - \omega_t - i\Gamma_n} , \tag{6}$$

where Γ_n is the damping of the level n. f_n and ω_n are the resulting exciton oscillator strengths and energies, respectively, which are influenced by the pump field directly and in contrast to the atomic Stark effect modified further by Coulomb interaction effects. The oscillator strengths are found to be

$$f_n = d_{cv}^2 \left[|\Psi_n(r=0)|^2 - 2\sum_{kk'} \psi_n(k)|\pi_{k'}^p|^2\psi_n^*(k') \right.$$
$$\left. - \sum_{kk'}\sum_{m\neq n} \frac{\psi_n(k)H_{nm}\psi_m^*(k') + (n \rightleftharpoons m)}{\omega_m^{(0)} - \omega_n^{(0)}} \right] , \tag{7}$$

with

$$H_{nm} = D_{nm} + \Delta_{nm} , \tag{8}$$

where

$$D_{nm} = 2d_{cv}E_p \sum_k \psi_n^*(k)(\pi_k^p)^*\psi_m(k) \tag{9}$$

and

$$\Delta_{nm} = 2\sum_{kk'} V_{k-k'}\psi_n^*(k)[(\pi_k^p)^* - (\pi_{k'}^p)^*]$$
$$\times [\pi_k^p\psi_m(k') + \pi_{k'}^p\psi_m(k)] . \tag{10}$$

The renormalized exciton energies are

$$\omega_n = \omega_n^{(0)} + D_{nn} + \Delta_{nn} . \tag{11}$$

III. APPLICATION TO SEMICONDUCTOR QUANTUM WIRES

For simplicity, let us consider a simple symmetry of a semiconductor quantum wire with circular cross section[9] of radius R. Extensions to wires of other symmetries with, e.g., rectangular or square cross sections are straightforward. By assuming an infinite quantum confinement in the lateral directions of the wire, one can carry out the averaging over the standing envelope states in the plane transverse to the wire axis z. Considering only the lowest wire subband reduces the Q1D exciton problem to an ideal 1D electron-hole Schrödinger equation with an effective Coulomb potential which depends on the wire radius R.[9,12] The explicit expression for such

an effective potential can be found, e.g., in Ref. 9. Here, we take the electron-hole Coulomb potential in the form[9]

$$U(z) = \frac{-e^2}{\epsilon_0(|z| + \lambda R)} . \tag{12}$$

ϵ_0 the static dielectric constant inside the wire. λ is a fitting parameter which is chosen to be 0.3 in order to fit the effective potential in Ref. 9. Note that Eq. (12) looks like the regularized Coulomb potential introduced by Loudon[8] but with the cutoff proportional to the wire radius, expressing an important physical connection.

Since the exciton wave functions are not explicitly available in momentum space, we cannot directly use the formulas given in the previous section. The exciton wave functions in real space[8] can be written as

$$\Psi_n^{(p)}(z) = [\theta(z) + (-1)^p\theta(-z)]N_n$$
$$\times W_{n,1/2}[2(\lambda R + |z|)/na] , \tag{13}$$

where $W_{n,1/2}(x)$ are the Whittaker functions,[16] and p specifies the parity state of the exciton ($p=0$ and 1 for even and odd states). a is the 3D exciton Bohr radius and N_n is the normalization coefficient given by

$$N_n = \frac{1}{\sqrt{an}} \frac{1}{\left[\int_{R_n}^\infty |W_{n,1/2}(x)|^2 dx\right]^{1/2}} . \tag{14}$$

Note that the integration in Eq. (14) is performed not from zero but from R_n to infinity, where R_n is proportional to the ratio between the wire radius and na. n is the energy quantum number:

$$R_n \equiv \frac{2\lambda R}{na} . \tag{15}$$

To evaluate the pump-induced level shifts and oscillator strength, we introduce as in Ref. 7 the following dimensionless quantities:

$$\rho_m = \Psi_n^*(z=0)\sum_k \psi_n(k)|\psi_m(k)|^2 , \tag{16}$$

$$\mu_m = \frac{|\Psi_n(z=0)|^2}{E_0}\sum_{kk'} V_{k-k'}\psi_n^*(k)[\psi_n^*(k) - \psi_n^*(k')]$$
$$\times [\psi_n(k)\psi_m(k') + \psi_n(k')\psi_m(k)] , \tag{17}$$

where E_0 is the 3D exciton Rydberg. ρ_m and μ_m are the enhancement factors of the Stark shift of a given exciton level m due to the anharmonic exciton-photon and exciton-exciton interactions, respectively. With a Fourier transformation for the exciton wave functions in momentum space, we have after a proper change of variables the following analytical expressions for the enhancement factors of the exciton ground state ρ_α, μ_α and of the band edge ρ_∞, μ_∞:

$$\rho_\alpha = \tfrac{1}{2}M_\alpha^4 W_{\alpha,1/2}(R_\alpha)\int_0^\infty dx\int_0^\infty dy\, W_{\alpha,1/2}(R_\alpha + x)W_{\alpha,1/2}(R_\alpha + y)[W_{\alpha,1/2}(R_\alpha + x + y) + W_{\alpha,1/2}(R_\alpha + |x-y|)] , \tag{18}$$

$$\mu_\alpha = \frac{2}{\alpha} M_\alpha^6 |W_{\alpha,1/2}(R_\alpha)|^2$$

$$\times \int_0^\infty dx \int_0^\infty dy \int_0^\infty dz\, u(z) W_{\alpha,1/2}(R_\alpha + x)$$

$$\times \{ W_{\alpha,1/2}(R_\alpha + z)[W_{\alpha,1/2}(R_\alpha + x + y) + W_{\alpha,1/2}(R_\alpha + |x - y|)]$$

$$- W_{\alpha,1/2}(R_\alpha + y)[W_{\alpha,1/2}(R_\alpha + x + z) + W_{\alpha,1/2}(R_\alpha + |x - z|)]\}$$

$$\times [W_{\alpha,1/2}(R_\alpha + y + z) + W_{\alpha,1/2}(R_\alpha + |y - z|)] , \tag{19}$$

$$\rho_\infty = M_\alpha^2 W_{\alpha,1/2}(R_\alpha) \int_0^\infty dx\, W_{\alpha,1/2}(R_\alpha + x) , \tag{20}$$

$$\mu_\infty = \frac{2}{\alpha} M_\alpha^4 |W_{\alpha,1/2}(R_\alpha)|^2 \left[2\int_0^\infty dx\, W_{\alpha,1/2}(R_\alpha + x)\int_0^\infty dy\, u(y)W_{\alpha,1/2}(R_\alpha + y) \right.$$

$$\left. - \int_0^\infty dx \int_0^\infty dy\, u(x)W_{\alpha,1/2}(R_\alpha + y)[W_{\alpha,1/2}(R_\alpha + x + y) + W_{\alpha,1/2}(R_\alpha + |x - y|)] \right] . \tag{21}$$

In Eqs. (18)–(21) α is the energy quantum number of the exciton ground state connected with the wire radius R by the following relation:[8]

$$\frac{1}{2\alpha} + \ln \left| \frac{2\lambda R}{\alpha a} \right| = 0 , \tag{22}$$

where $u(z)$ and M_α are given by

$$u(z) = \frac{1}{|z| + R_\alpha} \tag{23}$$

and

$$M_\alpha = \sqrt{a\alpha} N_\alpha . \tag{24}$$

With the aid of an integral representation for the Whittaker function for the exciton ground state $(0 \le \alpha < 1)$,

$$W_{\alpha,1/2}(x) = \frac{xe^{-x/2}}{\Gamma(1-\alpha)} \int_0^\infty dt\, e^{-xt} \left[1 + \frac{1}{t}\right]^\alpha , \tag{25}$$

we can numerically evaluate various enhancement factors, which are plotted in Fig. 1 as functions of wire radius. An interesting feature is that in the limit of small wire radius, μ_α and μ_∞ diverge as $1/\alpha$ [see Eqs. (19) and (21)], whereas ρ_α and ρ_∞ tend to the following finite values:

$$\lim_{R \to 0} \rho_\alpha = \frac{3}{2} , \tag{26}$$

$$\lim_{R \to 0} \rho_\infty = 2 . \tag{27}$$

These results can be obtained by using analytical properties of the Whittaker functions. The total Stark shifts of the exciton ground-state level $\Delta\omega_\alpha$ and of the band edge ΔE_g are given by

$$\frac{\Delta\omega_\alpha}{E_0} \equiv \frac{\omega_\alpha - \omega_\alpha^{(0)}}{E_0} = \left[\rho_\alpha + \frac{\mu_\alpha}{D}\right]\frac{I}{D} , \tag{28}$$

$$\frac{\Delta E_g}{E_0} \equiv \frac{E_g - E_g^{(0)}}{E_0} = \left[\rho_\infty + \frac{\mu_\infty}{D}\right]\frac{1}{D} , \tag{29}$$

where

$$D = \frac{|\omega_\alpha^{(0)} - \omega_p|}{E_0} \tag{30}$$

and

$$I = \frac{2|d_{cv}E_p|^2}{E_0^2} \tag{31}$$

are the scaled detuning and pump intensity, respectively, and $I = 1$ corresponds to an intensity of about 2 MW cm^{-2} for typical parameter values. The dependencies of the resulting shifts on R/a, D, and I are shown in Figs. 2 and 3. The figures show that the blueshifts are larger for thinner wires, stronger pumping, and smaller detuning. The exciton ground-state level at, e.g., $I = 4$ may be shifted to energies exceeding the unpumped band edge (see Fig. 2). For any values of wire radius R, pump intensity I, and detuning D, the band edge shifts by a larger amount than the exciton ground-state level does.
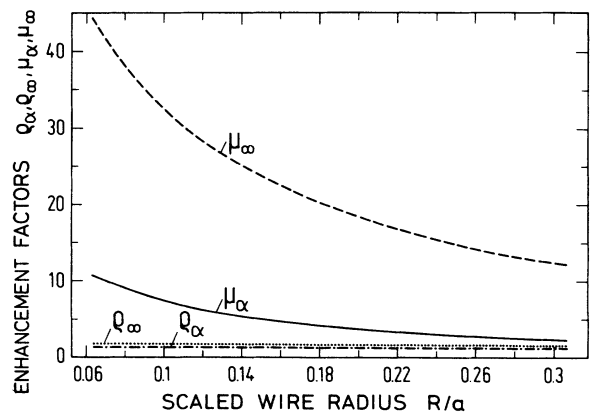

FIG. 1. Enhancement factors ρ_α, μ_α for the Q1D exciton ground-state level and ρ_∞, μ_∞ for the band edge as functions of scaled wire radius R/a.
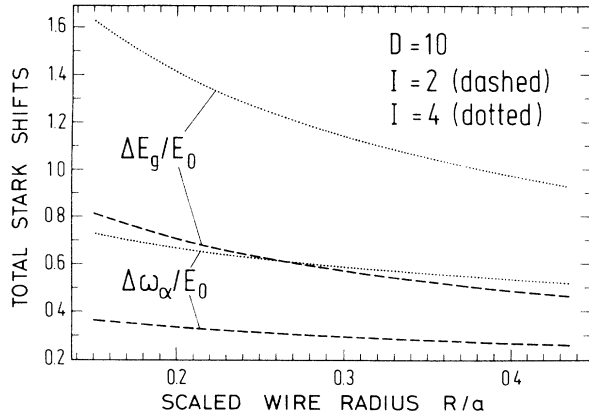
FIG. 2. Total Stark shifts $(\Delta\omega_\alpha)/E_0$ for the Q1D exciton ground-state level and $(\Delta E_g)/E_0$ for the band edge vs scaled wire radius R/a for scaled detuning $D=(|\omega_\alpha-\omega_p|)/E_0=10$ and different scaled pump intensities $I=2|d_{cv}E_p|^2E_0^2=2$ (dashed lines) and 4 (dotted lines).

This leads to an increase in the exciton binding energy similar to the 2D and 3D cases.[7]

We turn now to the calculation of the pump-induced changes of the oscillator strength for the Q1D exciton. To this end we need also to include in our consideration the excited states of the exciton. Because the exciton is strongly bound in low-dimensional systems, particularly in 1D (Q1D) systems, we shall take into account only the first excited level of the exciton whose main energy quantum number is denoted by β (to distinguish it from that of the ground state α). Following the approximate formula of Loudon,[8] we have

$$\beta\simeq1-\frac{1}{\ln\left[\dfrac{2\lambda R}{a}\right]}\tag{32}$$

and

$$\lim_{R\to0}\beta=1\ .\tag{33}$$
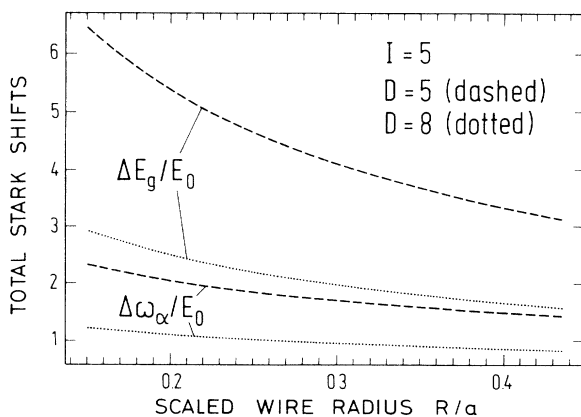

FIG. 3. Same as Fig. 2 but for $I=5$ and $D=5$ (dashed lines) and $D=8$ (dotted lines).
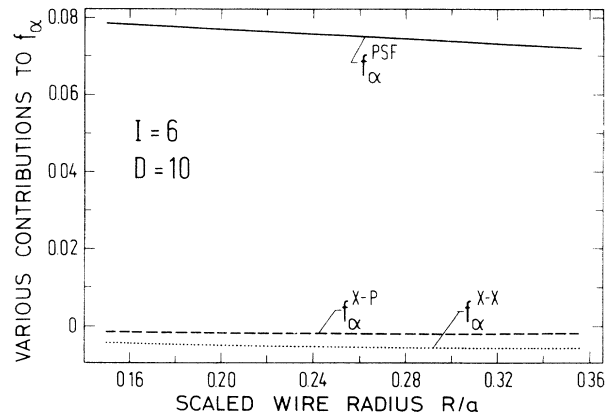

FIG. 4. Contributions to the exciton oscillator strength due to the phase-space filling effect (solid line), the exciton-photon interaction (dashed line), and the exciton-exciton interaction (dotted line). D and I are taken to be 10 and 6, respectively.

For the exciton wave function in the first excited state $(1\leq\beta<2)$ we have to use the following integral representation of the Whittaker function:

$$W_{\beta,1/2}(x)=\frac{xe^{-x/2}}{\Gamma(2-\beta)}\left[x\int_0^\infty dt\,e^{-xt}t\left(1+\frac{1}{t}\right)^\beta-\beta\int_0^\infty dt\,e^{-xt}\left(1+\frac{1}{t}\right)^{\beta-1}\right]\ .\tag{34}$$

In order to see clearly the various contributions to the total oscillator strength f_α, we split it into different parts f_α^{PSF}, f_α^{X-P}, and f_α^{X-X}, which are due to the phase-space filling effect, the exciton-photon and the exciton-exciton interactions, respectively:

$$f_\alpha=f_\alpha^{(0)}(1-f_\alpha^{\text{PSF}}-f_\alpha^{X-P}-f_\alpha^{X-X})\ .\tag{35}$$

For the unexcited case one has

$$f_\alpha\equiv f_\alpha^{(0)}=d_{cv}^2|\Psi_\alpha(z=0)|^2\ .\tag{36}$$
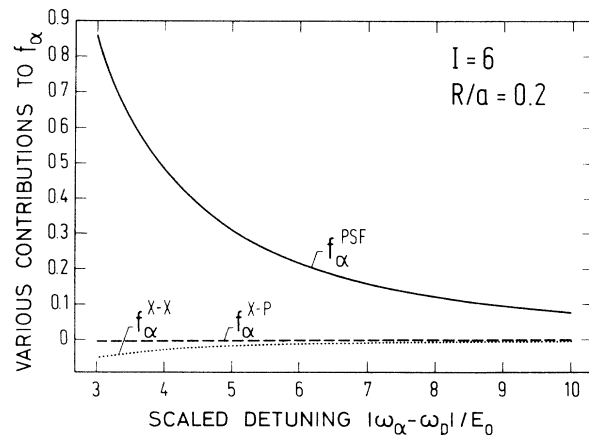

FIG. 5. Same as Fig. 4 but in dependence on scaled detuning D. I and R are taken to be 6 and $0.2a$, respectively.
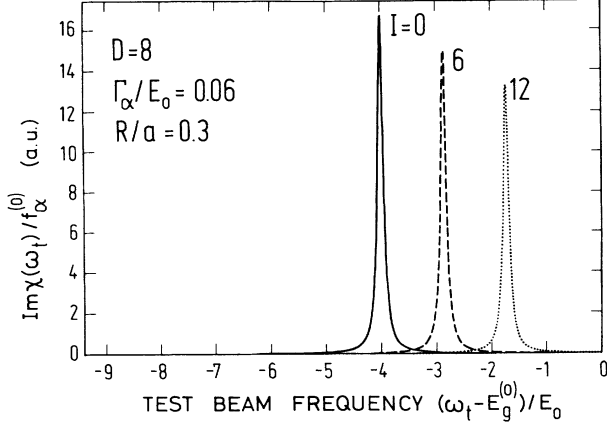
FIG. 6. $\mathrm{Im}\chi(\omega_t)/f_\alpha^{(0)}$ as functions of scaled frequency of the test beam $(\omega_t - E_g^{(0)})/E_0$ for $D=8$, $\Gamma_\alpha = 0.06E_0$, $R=0.3a$, and $I=0$ (solid curve), 6 (dashed curve), and 12 (dotted curve). The $I=0$ peak is located at -4, i.e., as were the position to the 2D exciton ground state, because we have taken $R=0.3a$, which corresponds to $\alpha = 0.5$ (following Loudon's formula) yielding $\omega_\alpha = -E_0/\alpha^2 = -4E_0$.

With a Fourier transformation for the exciton wave functions in both the ground state and the first excited state, we have obtained from Eq. (7) the following and analytical expressions:
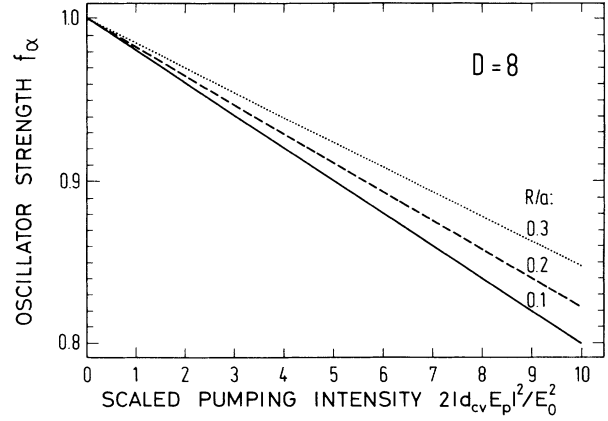

FIG. 7. Exciton oscillator strength as a function of the pump intensity for $D=8$ and $R=0.1a$ (solid line), $0.2a$ (dashed line), and $0.3a$ (dotted line).

$$f_\alpha^{\mathrm{PSF}} = \rho_\alpha \frac{I}{D^2} , \qquad (37)$$

$$f_\alpha^{X-P} = \frac{\alpha^3 \beta}{\beta^2 - \alpha^2} Q_{\alpha\beta} \frac{I}{D} , \qquad (38)$$

$$f_\alpha^{X-X} = \frac{\alpha^2 \beta}{\beta^2 - \alpha^2} P_{\alpha\beta} \frac{I}{D^2} , \qquad (39)$$

where

$$Q_{\alpha\beta} = M_\alpha^2 M_\beta^2 W_{\beta,1/2}(\alpha/\beta R_\alpha)$$

$$\times \int_0^\infty dx \int_0^\infty dy \, W_{\alpha,1/2}(R_\alpha + x) W_{\beta,1/2}[\alpha/\beta(R_\alpha + y)][W_{\alpha,1/2}(R_\alpha + x + y) + W_{\alpha,1/2}(R_\alpha + |x-y|)] , \qquad (40)$$

$$P_{\alpha\beta} = M_\alpha^4 M_\beta^2 W_{\alpha,1/2}(R_\alpha) W_{\beta,1/2}(\alpha/\beta R_\alpha)$$

$$\times \int_0^\infty dx \int_0^\infty dy \int_0^\infty dz \, u(z) W_{\alpha,1/2}(R_\alpha + x)[W_{\alpha,1/2}(R_\alpha + y + z) + W_{\alpha,1/2}(R_\alpha + |x-y|)]$$

$$\times (3W_{\alpha,1/2}(R_\alpha + z)\{W_{\beta,1/2}[\alpha/\beta(R_\alpha + x + y)] + W_{\beta,1/2}[\alpha/\beta(R_\alpha|x-y|)]\}$$

$$+ W_{\beta,1/2}[\alpha/\beta(R_\alpha + z)][W_{\alpha,1/2}(R_\alpha + x + y) + W_{\alpha,1/2}(R_\alpha + |x-y|)]$$

$$-4W_{\alpha,1/2}(R_\alpha + y)\{W_{\beta,1/2}[\alpha/\beta(R_\alpha + x + z)]$$

$$+ W_{\beta,1/2}[\alpha/\beta(R_\alpha + |x-z|)]\}) , \qquad (41)$$

and

$$M_\beta = \frac{1}{\left[\int_{R_\beta}^\infty |W_{\beta,1/2}(x)|^2 dx\right]^{1/2}} , \qquad (42)$$

with

$$R_{\beta} = \frac{\alpha}{\beta} R_\alpha . \qquad (43)$$

From Eqs. (37)–(39) it follows that $f_\alpha^{\mathrm{PSF}} \propto \rho_\alpha$ (ρ_α as already known is weakly dependent on wire radius and remains finite when R or α tend to zero), whereas

$f_\alpha^{X-P} \propto \alpha^3$ and $f_\alpha^{X-X} \propto \alpha^2$ will vanish in the limit of small wire radius. This means that in the Q1D systems the phase-space-filling effect plays a predominant role[15] as compared with the effects due to the exciton-photon and exciton-exciton interactions. In Figs. 4 and 5 we plot the various contributions to the total oscillator strength as functions of wire radius and detuning. One sees clearly the predominance of the phase-space-filling effect over the others. Figure 6 is the absorption spectrum of the test beam for three values of the pump intensity. Since the resulting oscillator strength f_α decreases with increasing pumping (see Fig. 7), it is predicted that the absorption peak should also decrease with pumping (Fig. 6).

IV. COMPARISON WITH 2D AND 3D CASES

The above derived results will now be compared with corresponding results of the 2D and 3D systems.[7] Qualitatively one finds in all three dimensions blueshifts of the exciton levels and an even larger blueshift of the band edge. However, the amounts of the shifts are distinctly different in the various dimensions. In Table I we show the numerical results for the Stark shifts. From the table we note that when dimensionality decreases, the anharmonic exciton-photon enhancement factors of the Stark shift ρ_α and ρ_∞ decrease, while the corresponding exciton-exciton enhancement factors μ_α and μ_∞ increase. The changes in ρ_α and ρ_∞ with the dimensionality can be expressed approximately in terms of the following relations:

$$\rho_\alpha^{(d)} \simeq \frac{2d+1}{2} , \tag{44}$$

$$\rho_\infty^{(d)} = 2^d , \tag{45}$$

where $d = 1$, 2, and 3 describes the dimension. The divergence of μ_α and μ_∞ as $1/\alpha$ (or $1/R$) in the limit of vanishing confinement length is a peculiar feature of purely 1D systems[8] due the singularity in the Coulomb potential. A qualitative distinction is obtained for the changes of the exciton ground-state oscillator strength in different dimensionalities. In the 3D structure, the contribution to f_α due to the phase-space-filling effect is always overcompensated for by those due to the exciton-photon and exciton-exciton interactions leading to a slight enhancement of f_α. On the other hand, the different contributions nearly quench each other in the dimension 2, resulting in almost total exciton oscillator strength which is nearly unaffected by the pump intensity. In contrast with both 3D and 2D situations, the contributions f_α^{X-P} and f_α^{X-X} vanish in the purely 1D case, and remain finite in the Q1D case, but they are very small as compared with f_α^{PSF} (see Figs. 4 and 5). The reduction of f_α is thus mainly due to the phase-space filling effect in 1D and Q1D systems. This dominance of the phase-space filling in Q1D, which has also been found in the plasma-density dependence of Q1D absorption spectra,[15] is the origin of the decrease of the absorption peaks with increasing pump intensity (Fig. 6).

The experience with bulk and quantum-well materials showed that in a pulsed experiment the resulting Stark shifts are considerably smaller, and the decrease of the

TABLE I. Numerical comparison between the various enhancement factors for the excitonic Stark level shifts in 3D, 2D, 1D, and Q1D systems.

	3D[a]	2D[a]	1D[b]	Q1D[b]
ρ_α	3.5	2.3	1.5	R dependent
ρ_∞	8	4	2	R dependent
μ_α	8.66	15.4	$\sim 1/\alpha$	R dependent
μ_∞	24	26.3	$\sim 1/\alpha$	R dependent

[a]Reference 7.
[b]This work.

oscillator strength is considerably larger than predicted by the calculations under stationary conditions. The advantage of the presented analysis for stationary pump and probe intensities is that it provides much more insight, e.g., into the dimensionality dependence of the various contributions in comparison with the purely numerical simulations of pulsed experiments. So far no experiments on the excitonic optical Stark effect in quantum wires have been reported, but such experiments will certainly be attempted as the quality of the quantum wires improves further.

APPENDIX A

This appendix gives a derivation of the normalization coefficient for the exciton wave function in a cylindrical quantum wire having circular cross section of radius R. The electron-hole Schrödinger equation in such a wire is of the form

$$\left[\frac{1}{2m_r}\frac{d^2}{dz^2} + \frac{e^2}{\epsilon_0(|z|+\lambda R)} + \omega_n \right]\Psi_n(z) = 0 , \tag{A1}$$

with m_r being the electron-hole reduced mass and $\omega_n = -E_0/n^2$. With the variable changes

$$z \to z' = \frac{2}{an}(\lambda R + z) \tag{A2}$$

for $z > 0$, and

$$z \to z' = \frac{-2}{an}(\lambda R - z) \tag{A3}$$

for $z < 0$, Eq. (A1) becomes

$$\left[\frac{d^2}{dz'^2} - \frac{1}{4} + \frac{n}{z'} \right]\Psi_n(z') = 0 . \tag{A4}$$

(A4) is Whittaker's form of the confluent hypergeometric equation. For $z' > 0$, one of the two linearly independent solutions of (A4) which vanishes in the limit $z' \to \infty$ is $W_{n,1/2}(z')$. In this case the exciton bound-state wave function can be written as

$$\Psi_n(z) = N_n W_{n,1/2}[2/(an)(\lambda R + z)] , \tag{A5}$$

where N_n is some normalization constant to be determined later on. On the other hand, for $z' < 0$, the solution of (A4) that tends to zero for large z' is $W_{n,1/2}(-z')$. In this case the exciton wave function is of the form

$$\Psi_n = N_n' W_{n,1/2}[2/(an)(\lambda R - z)] , \tag{A6}$$

where N_n' is another constant which is in general different

from N_n given in (A5). However, because at $z=0$ the functions defined by (A5) and (A6) should be joined together, i.e.,

$$N_n W_{n,1/2}(2\lambda R/an) = N_n' W_{n,1/2}(2\lambda R/an) , \qquad (A7)$$

we find

$$N_n \equiv N_n' . \qquad (A8)$$

The normalization condition for the exciton wave function requires

$$1 = \int_{-\infty}^{\infty} dz |W_{n,1/2}(z)|^2$$

$$= N_n^2 \left[\int_{-\infty}^{0} dz |W_{n,1/2}[2/(an)(\lambda R - z)]|^2 \right.$$

$$\left. + \int_{0}^{\infty} dz |W_{n,1/2}[2/(an)(\lambda R + z)]|^2 \right] . \qquad (A9)$$

In the first integral of (A9) we change variable as $z \to x = 2/(an)(\lambda R - z)$ and have

$$\int_{-\infty}^{0} dz |W_{n,1/2}[2/(an)(\lambda R - z)]|^2$$

$$= \frac{an}{2} \int_{R_n}^{\infty} dx |W_{n,1/2}(x)|^2 , \qquad (A10)$$

whereas in the second integral the change of variable is $z \to x = 2/(an)(\lambda R + z)$ and gives

$$\int_{0}^{\infty} dz |W_{n,1/2}[2/(an)(\lambda R + z)]|^2$$

$$= \frac{an}{2} \int_{R_n}^{\infty} dx |W_{n,1/2}(x)|^2 . \qquad (A11)$$

(A10) and (A11) together with (A9) yields the analytical expression for N_n of Eqs. (13) and (14).

APPENDIX B

In this appendix we shall derive Eqs. (18)–(21) and prove the limits given in Eqs. (26) and (27). From the general theory[1] one has

$$\rho_\alpha = \Psi_\alpha^*(z=0) \sum_k \psi_\alpha(k) |\psi_\alpha(k)|^2 , \qquad (B1)$$

$$\rho_\infty = \Psi_\alpha^*(z=0)\psi_\alpha(k=0) . \qquad (B2)$$

Applying the Fourier transformation

$$\psi_\alpha(k) = \int_{-\infty}^{\infty} dz\, e^{ikz}\Psi_\alpha(z) , \qquad (B3)$$

we cast (B1) and (B2) into

$$\rho_\alpha = \Psi_\alpha^*(z=0)\int_{-\infty}^{\infty} dx' \int_{-\infty}^{\infty} dy' \Psi_\alpha(x')\Psi_\alpha(y')$$

$$\times \Psi_\alpha(y'-x') , \qquad (B4)$$

$$\rho_\infty = \Psi_\alpha^*(z=0)\int_{-\infty}^{\infty} dx' \Psi_\alpha(x') . \qquad (B5)$$

Using Eqs. (13) and (24) we can, after changing variables as $2x'/\alpha a \to x$ and $2y'/\alpha a \to y$, rewrite (B4) and (B5) in terms of Whittaker functions as

$$\rho_\alpha = \tfrac{1}{4}M_\alpha^4 W_{\alpha,1/2}(R_\alpha)$$

$$\times \int_{-\infty}^{\infty} dx \int_{-\infty}^{\infty} dy\, W_{\alpha,1/2}(R_\alpha + |x|)$$

$$\times W_{\alpha,1/2}(R_\alpha + |y|)$$

$$\times W_{\alpha,1/2}(R_\alpha + |y - x|) , \qquad (B6)$$

$$\rho_\infty = \tfrac{1}{2}M_\alpha^2 \int_{-\infty}^{\infty} dx\, W_{\alpha,1/2}(R_\alpha + |x|) . \qquad (B7)$$

Transforming the integrations in (B6) and (B7) from $-\infty$ to ∞ into those from 0 to ∞, we get immediately Eqs. (18) and (20). Equations (19) and (21) can also be derived in a similar manner. Note that the $1/\alpha$ dependence in (19) and (21) arises from the appropriate change of variables in the Coulomb potential, namely $2z/\alpha a \to z$, which casts $U(z) = -e^2/\epsilon_0(|z| + \lambda R)$ in Eq. (12) into $-4E_0/\alpha u(z)$, with $u(z)$ being defined by Eq. (23). Thus the divergence in μ_α and μ_∞ as $1/\alpha$ is due to the singularity in the Coulomb potential when the ideal 1D limit is approached.

Now we shall prove the limits Eqs. (26) and (27). For this purpose we invoke the following property of the Whittaker function:[16]

$$\lim_{\alpha \to 0} W_{\alpha,1/2}(x) \equiv W_{0,1/2}(x) = e^{-x/2} . \qquad (B8)$$

Then, from Eqs. (18), (20), (24), (14), and (B8), we have

$$\lim_{\alpha \to 0}\rho_\alpha = \frac{1}{2}\frac{e^{-R_\alpha/2}}{\left[\int_{R_\alpha}^{\infty} dx\, e^{-x}\right]^2}\int_0^{\infty} dx \int_0^{\infty} dy\, e^{-(R_\alpha + x)/2}e^{-(R_\alpha + y)/2}(e^{-(R_\alpha + x + y)/2} + e^{-(R_\alpha + |x - y|)/2})$$

$$= \frac{1}{2}\left[\int_0^{\infty} dx\, e^{-x}\int_0^{\infty} dy\, e^{-y} + \int_0^{\infty} dx\, e^{-x/2}\int_0^{\infty} dy\, e^{-(y + |x - y|)/2}\right]$$

$$= \frac{1}{2}\left[1 + \int_0^{\infty} dx\, e^{-x/2}\left[\int_0^{x} dy\, e^{-(y + x - y)/2} + \int_x^{\infty} dy\, e^{-(y - x + y)/2}\right]\right]$$

$$= \frac{1}{2}\left[1 + \int_0^{\infty} dx\, xe^{-x} + \int_0^{\infty} dx\, e^{-x}\right] = \tfrac{3}{2} \qquad (B9)$$

and

$$\lim_{\alpha\to 0}\rho_\infty = \frac{e^{-R_\alpha/2}}{\int_{R_\alpha}^\infty dx\, e^{-x}} \int_0^\infty dx\, e^{-(R_\alpha+x)/2} = 2\int_0^\infty dy\, e^{-y} = 2 \ . \tag{B10}$$

Since R also vanishes when α tends to zero, (B9) and (B10) are nothing else but Eqs. (26) and (27), respectively.

*On leave of absence from the Institute of Theoretical Physics, P.O. Box 429 Boho, Hanoi 10000, Vietnam.

[1] For a fairly recent introduction, see *Quantum Theory of the Optical and Electronic Properties of Semiconductors*, edited by H. Haug and S. W. Koch (World Scientific, Singapore, 1990). Several reviews on low-dimensional systems are contained in *Optical Switching in Low-Dimensional Systems*, Vol. 144 of *NATO Advanced Study Institute Series B: Physics*, edited by H. Haug and L. Banyai (Plenum, New York, 1989).

[2] See, e.g., W. H. Knox, C. Hirlimann, D. A. B. Miller, J. Shah, D. S. Chemla, and C. V. Shank, Phys. Rev. Lett. **56**, 1191 (1986).

[3] A. Mysyrowicz, D. Hulin, A. Antonetti, A. Migus, W. T. Masselink, and H. Morkoç, Phys. Rev. Lett. **56**, 1335 (1985).

[4] A. Von Lehmen, J. E. Zucker, J. P. Heritage, and D. S. Chemla, Opt. Lett. **11**, 609 (1986).

[5] S. Schmitt-Rink, D. S. Chemla, and H. Haug, Phys. Rev. B **37**, 941 (1988).

[6] S. W. Koch, N. Peyghambarian, and M. Lindberg, J. Phys. C **21**, 5229 (1988).

[7] C. Ell, J. F. Müller, K. El Sayed, and H. Haug, Phys. Rev. Lett. **62**, 304 (1989).

[8] R. Loudon, Am. J. Phys. **27**, 649 (1959).

[9] L. Banyai, I. Galbraith, C. Ell, and H. Haug, Phys. Rev. B **36**, 6099 (1987).

[10] L. Banyai, I. Galbraith, and H. Haug, Phys. Rev. B **38**, 3931 (1988).

[11] S. Abe, J. Phys. Soc. Jpn. **58**, 62 (1990).

[12] T. Ogawa and T. Takagahara, Phys. Rev. B **43**, 14325 (1991); **44**, 8138 (1991).

[13] H. Sakaki, K. Kato, and H. Yoshimura, Appl. Phys. Lett. **57**, 2800 (1990).

[14] H. Ando, H. Oochashi, and H. Kanbe, J. Appl. Phys. **70**, 7024 (1991).

[15] S. Benner and H. Haug, Europhys. Lett. **16**, 579 (1991).

[16] I. S. Gradshteyn, and I. M. Ryzhik, *Table of Integrals, Series and Products* (Academic, New York, 1965).